IS-T--1437

DE90 011747

Selective Electrocatalysis of Anodic Oxygen-transfer Reactions at Chemically Modified, Thin-film Lead Dioxide Electrodes

by

Hsiangpin Chang

PHD Thesis submitted to Iowa State University

Ames Laboratory, U.S. DOE
Iowa State University
Ames, Iowa 50011

Date Transmitted: January 1990

PREPARED FOR THE U. S. DEPARTMENT OF ENERGY
UNDER CONTRACT NO. W-7405-Eng-82.

Selective electrocatalysis of anodic oxygen-transfer reactions at chemically modified, thin-film lead dioxide electrodes[1]

Hsiangpin Chang

Under the supervision of Dennis C. Johnson
From the Department of Chemistry
Iowa State University

The strategy to modify PbO_2 electrodes for electrocatalysis of oxygen-transfer (O-t) reactions is to incorporate spatially separated catalytic sites into the PbO_2 surface. The rate of ·OH radical formation is promoted at these sites, as is the rate of the O-t reaction, for the latter was demonstrated to be proportional to the former.

The electrodeposition of PbO_2 was studied as a special case of a heterogeneous O-t reaction. Soluble Pb(IV) species were detected with a rotated ring-disc electrode as intermediate products of the PbO_2 deposition. These unstable Pb(IV) species are partially responsible for the catalytic activities of in-situ deposited PbO_2 electrode, as studied by voltammetry, spectrophotometry, and flow-injection analysis.

Chemically modified PbO_2 is electrodeposited by addition of Bi^{3+}, As(III), or Cl^- to the Pb^{2+} plating bath. The electrochemical stability and catalytic activity of the Bi-doped PbO_2 (Bi-PbO_2) increase with increased Bi/Pb atomic ratio in the mixed oxide which were determined by X-ray photoelectron spectroscopy.

Microcracked, ultra-thin films of Bi-PbO_2 were found at Au, Pt, GC,

---

[1] This work was performed in Ames Laboratory under Contract No. W-7405-Eng-82 with the U. S. Department of Energy.

and Ti electrodes after consecutive deposition and stripping of the thick oxide films. The ultra-thin film has higher catalytic activity and stability than the original film, due to an enhanced Bi surface concentration. The morphology and structure of the ultra-thin films were studied by scanning electron microscope and X-ray diffraction.

The surface of pure PbO_2 can be modified by Bi^{3+}, As(V), and Cl^- by electroadsorption. The adsorption method to modify PbO_2 is fast and efficient for screening new catalysts. The catalytic activity of Bi^{3+}-adsorbed PbO_2 was determined to result in well-defined, mass transport-limited voltammetric plateaus for the anodic reactions $Mn^{2+} \rightarrow MnO_4^-$, $Cr^{3+} \rightarrow CrO_4^-$, $(CH_3)_2SO \rightarrow (CH_3)_2SO_2$, and $(CH_2)_4SO \rightarrow (CH_2)_4SO_2$. The $E_{1/2}$ values for these varied processes are virtually the same. The $E_{1/2}$ values are a function of the surface concentration of the catalyst and only slightly influenced by the identity of the catalyst.

An O-t mediation mechanism was proposed for the electrocatalysis observed at the chemically modified PbO_2. The catalysts serve as O-t mediators, which are different from electron-transfer mediators by not undergoing any redox change during the catalysis.

Selective electrocatalysis of anodic oxygen-transfer reactions at chemically modified, thin-film lead dioxide electrodes

by

Hsiangpin Chang

A Dissertation Submitted to the
Graduate Faculty in Partial Fulfillment of the
Requirements for the Degree of
DOCTOR OF PHILOSOPHY

Department: Chemistry
Major: Analytical Chemistry

Approved:

In Charge of Major Work

For the Major Department

For the Graduate College

Iowa State University
Ames, Iowa

1989

TABLE OF CONTENTS

* copyrighted papers removed and cycled separately.

LIST OF MAJOR SYMBOLS AND ABBREVIATIONS

$Bi\text{-}PbO_2$ - bismuth-doped lead dioxide
Bi^{3+}/PbO_2 - bismuth(III)-adsorbed lead dioxide
DMSO - dimethyl sulfoxide
$DMSO_2$ - dimethyl sulfone
$E°$ - standard potential
$E_{1/2}$ - half-wave potential
EDS - X-ray energy dispersive spectroscopy
e-t - electron-transfer
FI-EC - flow injection with electrochemical detector
GC - glassy carbon
GC/MS - gas chromatography/mass spectrometry
O-t - oxygen-transfer
RDE - rotating disc electrode
RRDE - rotating ring-disc electrode
SCE - saturated calomel electrode
SEM - scanning electron microscope
TMSO - tetramethyl sulfoxide
TPCA - 2-thiophene carboxylic acid
XPS - X-ray photoelectron spectroscopy
XRD - X-ray diffraction
ϕ - scan rate
w - rotational velocity
v - kinematic viscosity

DEDICATION

To my beloved parents and my dearest wife:

Duan Qiongyin, Chang Qingshu, and Chang S. Suichu

I. GENERAL INTRODUCTION

A. Strategies to Modify Lead Dioxide Electrodes Selectively for Catalysis of Anodic Oxygen-Transfer Reactions

"The last word of 'analytical chemistry' is *chemistry*."

-Dennis C. Johnson

What are anodic oxygen-transfer reactions?

An anodic oxygen-transfer (O-t) reaction is defined as a reaction that involves the transfer of oxygen from the solvent (H_2O) to the reactant R, which can be written in general as follows:

$$R + H_2O \xrightarrow{\text{electrode}} RO + 2\ H^+ + 2\ e \qquad [1]$$

This type of reaction differs from simple electron-transfer (e-t) reactions, e.g., $Fe^{2+} = Fe^{3+} + e$. The O-t reactions are more complicated than e-t reactions because of the coupling of proton- and oxygen-transfer steps with the transfer of electrons. The O-t reactions in acidic media are usually characterized by slow heterogeneous kinetics at conventional electrodes because of the additional process of activation of the oxygen from water. It has been concluded that, generally, anodic O-t reactions can occur only via chemical participation of some electrode surface species, e.g., a labile, adsorbed hydroxyl radical generated during anodic surface oxide formation or water discharge (1). Unfortunately, these labile surface hydroxyl species are not readily available at the conventional solid electrodes commonly used as anodes. In order to use the anodic O-t reactions efficiently for practical applications, e.g., in electroorganic synthesis, fuel cells, and anodic amperometric detection, it is necessary to search for new electrode materials with selective, catalytic activity for O-t reactions.

Some typical anodic O-t reactions of practical importance are listed in Table 1. The production of perchlorate, benzoquinone, and anthroquinone are significant for commercial electrosynthesis (2). The

Table 1. Examples of Oxygen-Transfer Reactions

$H_2O + SO_3^{2-} \longrightarrow SO_4^{2-} + 2H^+ + 2e$

$CO \longrightarrow CO_2$

$Cl^- \longrightarrow ClO_3^- \longrightarrow ClO_4^-$

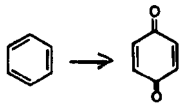

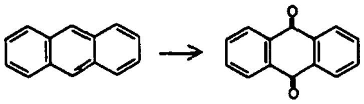

$Cr^{3+} \longrightarrow Cr_2O_7^{2-}$

$(CH_3)_2SO \longrightarrow (CH_3)_2SO_2$ (E° = 0.0 V vs. SCE)

$Mn^{2+} \longrightarrow MnO_4^-$ (E° = 1.3 V)

---

oxidation of Cr(III) to chromic acid, and Mn(II) to permanganate, are used in indirect oxidative electrolyses (3).

Throughout this research, the oxidation of dimethyl sulfoxide (DMSO) to dimethyl sulfone ($DMSO_2$) is used as the primary model O-t reaction. It was chosen because it is a one-oxygen-transfer reaction with a simple oxidation product which is soluble in aqueous solution. The oxidation of Mn(II) to MnO_4^- was chosen as a secondary model reaction because its product has intense color and so can be monitored easily with a spectrophotometric detector. The characteristic slow kinetics of anodic O-t reactions is well represented by these two reactions in spite of their relatively low values of standard potential, 0.0 V and 1.35 V (4), respectively. Additional reactions from Table 1 were also studied. It was hoped that electrodes that tested positive for electrocatalysis with the model reactions would work virtually the same for other O-t reactions because all anodic O-t reactions share the same kinetic barrier.

<u>Why do we need to modify lead dioxide electrodes?</u>

Firstly, it has been a common perception that pure lead dioxide electrode lacks specific catalytic activities despite its wide use for anodic electrosynthesis (5). The common choice of PbO_2 as an anodic material for large-scale anodic electrosynthesis has been based, apparently, on the knowledge of the very large overpotential for oxygen evolution at pure PbO_2 and the impression that the accessibility of a large positive potential with minimal background current can adequately drive slow anodic reactions. Provided the above premise is correct, that anodic O-t reactions are electrocatalyzed by mechanistic coupling with the process of oxygen evolution, then the common strategy is seen to be without rational foundation. It is believed that properly modified PbO_2 electrodes with specific catalytic activity can play an important role in many practical electrochemical processes.

Secondly, the initial screening of electrode materials indicated that lead dioxide might be particularly appropriate for O-t reactions following modification of the bulk and/or surface structure of the oxide by incorporation of alternate metals for the lead. From previous studies of O-t reactions at noble metal electrodes, e.g., Au and Pt (1), it is known that the surfaces of metal oxides can be active participants in the electrocatalysis of anodic O-t reaction. However, O-t reactions at the noble metal electrodes lack long-term stability under constant-potential or constant-current conditions because of the passivation of the electrode surface which depresses the formation of the surface-bound state of active oxygen. It is anticipated that bulk oxide electrodes, e.g., PbO_2, should be better electrodes for O-transfer than the noble metals, because they are "oxygen-rich" at the surfaces (6). This is proved by the moderate catalytic activity of pure PbO_2 for the oxidation of some sulfur compounds (6a-c) and I^- to IO_4^- (7). It is also predicted that the catalytic activity of PbO_2 will be enhanced by proper chemical modification, specifically incorporation of foreign species as catalysts.

Thirdly, lead dioxide is believed to be readily suitable for chemical modification. It is a non-stoichiometric dioxide, with formulae of PbO_x ($x = 1.9 - 2.0$) (5). Thus, it should be possible to incorporate foreign ionic species into PbO_2 matrix by electrodeposition (6b-e).

The surface defects of PbO_2 can also contribute to chemisorption and catalysis (8a). In addition, the surface structure of most metal oxides can be considered at atomic level as either terminated OH species or bridged O species (8b-d):

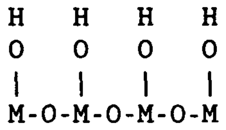

(terminated OH)

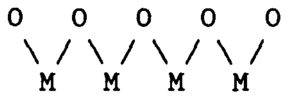

(bridiged O)

The actual picture undoubtedly is more complex, being some combination of both. In any case, some ion exchange or complexation ability of the oxide surface exists, which can be used to chemisorb ionic species as catalytic agents and thus to modify the surfaces of lead dioxide.

Finally, from practical points of view, lead dioxide was chosen because of its high electric conductivity, ease and low cost of preparation, chemical inertness to both acidic and alkaline media, stability at high temperatures, and high oxygen overpotential. The fundamental research of chemically modified electrodes has received great success in the last decade. However, the electrode materials tested have been mainly organic polymers and have not been accepted in large-scale electrolysis because of their lack of chemical inertness and stability. It is hopeful that the development of inorganic, modified PbO_2 electrodes will change this situation.

How to modify PbO_2 electrodes selectively for catalysis of anodic O-transfer reactions?

To answer this question, the mechanism of O-t reaction is considered first in relation with that of anodic oxygen evolution. It is generally believed (9) that the first and rate-limiting step for the anodic evolution of oxygen is the discharge of water to yield the hydroxyl radical (·OH) which is adsorbed at the electrode (M), as shown in Figure 1. The adsorbed hydroxyl radicals are further oxidized to give dioxygen and regenerate the M surface. If an oxidizable reactant R is present in the solution, the hydroxyl can be transferred to R to produce the oxidation product RO, which is indicated by the wide arrows in Figure 1.

It is, thus, clear that the electrocatalysis of O-t reactions can be achieved by simultaneous promotion of the rate of hydroxyl generation and depression of the rate of oxygen evolution. This can be done by incorporation onto the PbO_2 surface of a material with a low oxygen-evolution overpotential as catalyst in such a way that the catalytic sites are well separated from each other. Therefore, they serve as centers to generate the ·OH species yet with a relatively low yield of oxygen gas. This strategy is illustrated schematically in Figure 2. Since PbO_2 (A) has a high oxygen overpotential and the coverage of the catalyst (B) on PbO_2 is low, the modified PbO_2 should have a similar, if not the same, low value of oxygen overpotential to that of the pure PbO_2. Yet the activity for the anodic O-t reaction at the modified PbO_2 should be increased greatly without losing the advantages, e.g., low background signal, of the pure PbO_2 electrode. The resultant chemically modified

PbO_2 electrode can be regarded as a partially covered or a so-called "array" electrode (10). With appropriate surface coverage of the catalyst, the O-t reaction at these electrodes should proceed quickly and under mass-transport control. However, it is expected that if the coverage is too high, the catalytic activity for the O-t reaction will decrease because the catalysts at the electrode surface will no longer be separated from each other, so a high background signal for oxygen evolution will arise.

Selection of catalysts

The potential catalysts for PbO_2 modification should be the ones that have low values of oxygen overpotential. There has been a large body of literature on the studies of oxygen-evolution as a function of electrode materials. Most important to the present study is the work by Trassatti (11) and other workers who tried to correlate the oxygen overpotential to the enthalpy of the oxide transition. The corresponding plots have a peaked shape, with large overpotential for both small and large transition enthalpy, and a minimum overpotential for an intermediate transition enthalphy. Because of their cone shape, the plots have been referred to as "volcano plots." Based on this correlation, some doping agents can be selected initially to test (6d,e). However, the use of the volcano plot to anticipate potential catalysts has limitations. For instance, the values of heat of formation used for the plots are only for oxides of two oxidation states. Nevertheless, the catalysts incorporated into the PbO_2 may not necessarily exist in a pure oxide form or may not easily change in oxidation state. An additional difficulty is that the metal ions chosen from the volcano plots might not be incorporated readily into or onto the PbO_2 surface. Therefore, the selection of the catalysts in this study was done empirically. Attention was, however, paid to develop techniques to reduce the burden of repetitive work for the screening of catalysts out of a large number of candidates.

It was also hoped that more than one catalyst can be found, so the identity of the catalysts can be varied to yield information pertaining to the mechanism of the electrocatalysis.

Scope of research

The scope of this research is summarized as follows:

(1) Development of efficient methods for chemical modification of lead dioxide electrodes and selection of catalysts for electrocatalysis of anodic O-t reactions;

(2) Characterization of the resultant catalytic electrode materials;

(3) Understanding of the kinetics and mechanism of the electrocatalysis.

Experimental configurations

Thin-film PbO_2 electrodes (ca. 10 - 50 μm) electrodeposited on Au or other substrates were used throughout this study, primarily because of the convenience in electrode preparation. It will be proved that the actual behavior of the modified PbO_2 electrodes does not change with the thickness of the oxide films.

Most of the studies were done in acidic media, specifically

$HClO_4$ solutions, because $HClO_4$ is a non-chelating acid.

The basic electrochemical techniques used are hydrodynamic voltammetry and chronoamperometry in conventional electrolysis cells. Exhaustive electrolysis at large-area screen electrodes was used for experimental upgrading. Flow-through systems, visible spectrophotometry, and gas chromatography with mass spectrometric detection were also used for special purposes. Some techniques for surface and structure analysis, e.g., X-ray diffraction (XRD), X-ray photoelectron spectroscopy (XPS), scanning electron microscopy (SEM), and X-ray energy-dispersive spectroscopy (EDS), were used to characterize the morphology, composition, and structure of the modified PbO_2 films.

References

1. (a) Johnson, D. C. J. Electrochem. Soc. 1972, 119, 331. (b) Austin, D. S.; Johnson, D. C.; Hines, T. G.; Berti, E. T. Anal. Chem. 1983, 55, 2222. (c) Cabelka, T. D.; Austin, D. S.; Johnson, D. C. J. Electrochem. Soc. 1984, 131, 1596; 1985, 132, 359.

2. (a) Seltzer, R. J. C&EN, August 8, 1988; p. 13. (b) Aprem, M. M.; Unnikrishnan, K.; Sukumaran, K. M.; Nair, K. S. Trans. SAEST, 1985, 20, 201.

3. (a) Steckhan, E. Top. Curr. Chem. Electrochemistry, Volume 1; Stechhan, E., Ed.; Springer-Verlag: Berlin, 1987. (b) Ibl, N.; Kramer, K.; Ponto, L.; Robertson, P. In "Electro-organic Synthesis Technology"; Krumpelt, M; Weissman, E. V.; Alkire, R. C., Eds.; AIChE Symposium Series, Vol. 75, No. 185, New York, 1979.

4. "Standard Potentials in Aqueous Solutions"; Bard, A. J.; Parson, R.; Jordan, J., Eds.; M. Dekker: New York, 1985.

5. Carr, J. P.; Hampson, N. A. Chem. Rev. 1972, 72, 679.

6. (a) Tang, A. P.-C.; Johnson, D. C. Anal. Chim. Acta In press. (b) Austin, D. S.; Polta, J. A.; Polta, T. Z.; Tang, A. P.-C.; Cabelka, T. P.; Johnson, D. C. J. Electroanal. Chem. 1984, 168, 227. (c) Johnson, D. C.; Polta, J. A.; Polta, T. Z.; Neuburger, G. G.; Johnson, J.; Tang, A. P.-C.; Yeo, I.-H.; Baur, J. J. Chem. Soc.,

Faraday Trans. 1, 1986, 82, 1081. (d) Yeo, I.-H.; Johnson, D. C. J. Electrochem. Soc. 1987, 134, 1973. (e) Yeo, I.-H. Ph.D. Dissertation, Iowa State University, Ames, Iowa, 1987.

7. Hampel, C. A. "The Encyclopedia of Electrochemistry"; Chapman & Hall: London, 1964; p. 763.

8. (a) Henrich, V. E. In "Surface and Near-Surface Chemistry of Oxide Mateirals"; Nowotny, J.; Dufour, L.-C., Eds.; Elsevier: Amsterdam, 1988; Chapter 2, p. 23. (b) Hall, W. K. In "Chemistry and Physics of Solid Surfaces VI"; Vanselow, R.; Howe, R., Eds.; Springer-Verlag: Berlin, 1986; Chapter 5, p. 73. (c) Ruvarac, A. In "Inorganic Ion Exchange Materials"; Clearfield, A., Ed.; CRC Press: Boca Raton, 1982; Chapter 5, p. 141. (d) Abe, M. In "Inorganic Ion Exchange Materials"; Clearfield, A., Ed.; CRC Press: Boca Raton, 1982; Chapter 6, p. 275.

9. (a) Tarasevich, M. R.; Sadkowski, A.; Yeager, E. In "Comprehensive Treatise of Electrochemistry," Conway, B. E.; Bockris, J. O'M.; Yeager, E.; Khan, S. U. M.; White, R. E., Eds.; Plenum Press: New York, 1983; Volume 7, p. 301. (b) O'Sullivan, E. J. O'M.; Calvo, E. J. In "Comprehensive Chemical Kinetics," Compton, R. G., Ed.; Elsevier: Amsterdam, 1987; Volume 27, p. 247.

10. (a) Caprani, A.; Deslouis, C.; Robin, S.; Tribollet, B. J. Electroanal. Chem. 1987, 238, 67. (b) Levart, E. J. Electroanal. Chem. 1985, 187, 247. (c) Amatore, C.; Saveant, J. M.; Tessier, D. J. Electroanal. Chem. 1983, 147, 39. (d) Contamin, O.; Levart, E. J. Electroanal. Chem. 1982, 136, 259. (e) Gueshi, T.; Tokuda, K.; Matsuda, H. J. Electroanal. Chem. 1979, 101, 29; 1978, 89, 247. (f) Tokuda, K.; Gueshi, T.; Matsuda, H. J. Electroanal. Chem. 1979, 102, 41. (g) Filinovsk, V. Yu. Electrochim. Acta 1979, 25, 309.

11. Trasatti, S. J. Electroanal. Chem. 1980, 111, 125.

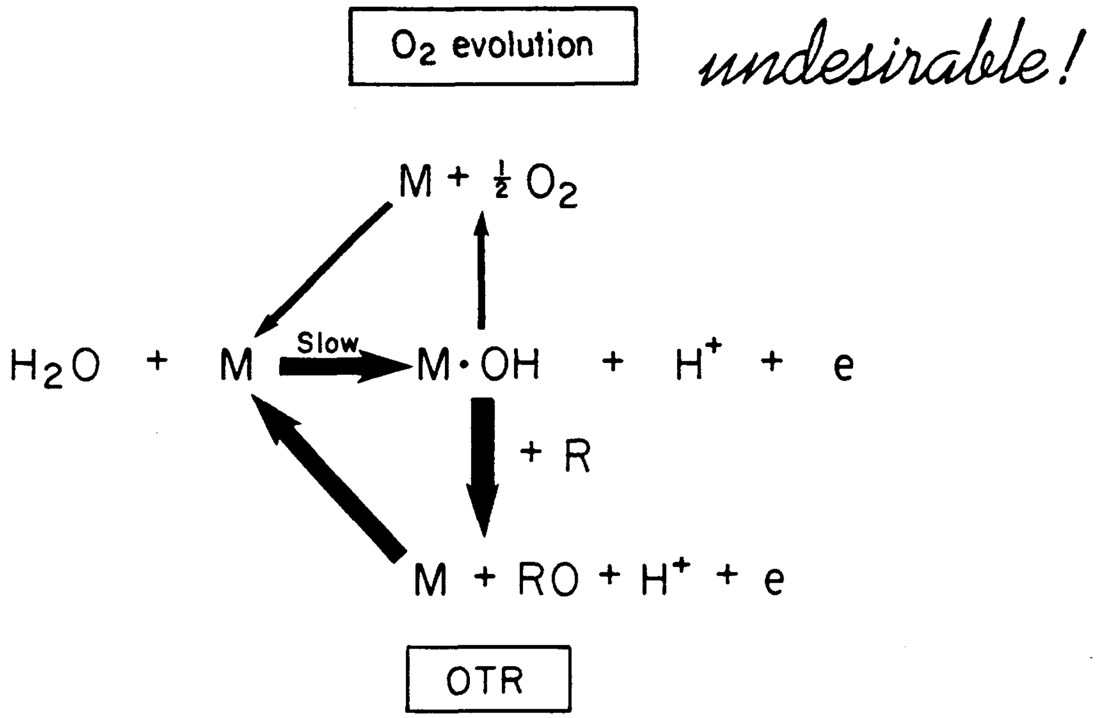

Figure 1. Schematic diagram for the mechanism of oxygen evolution and oxygen-transfer mediation

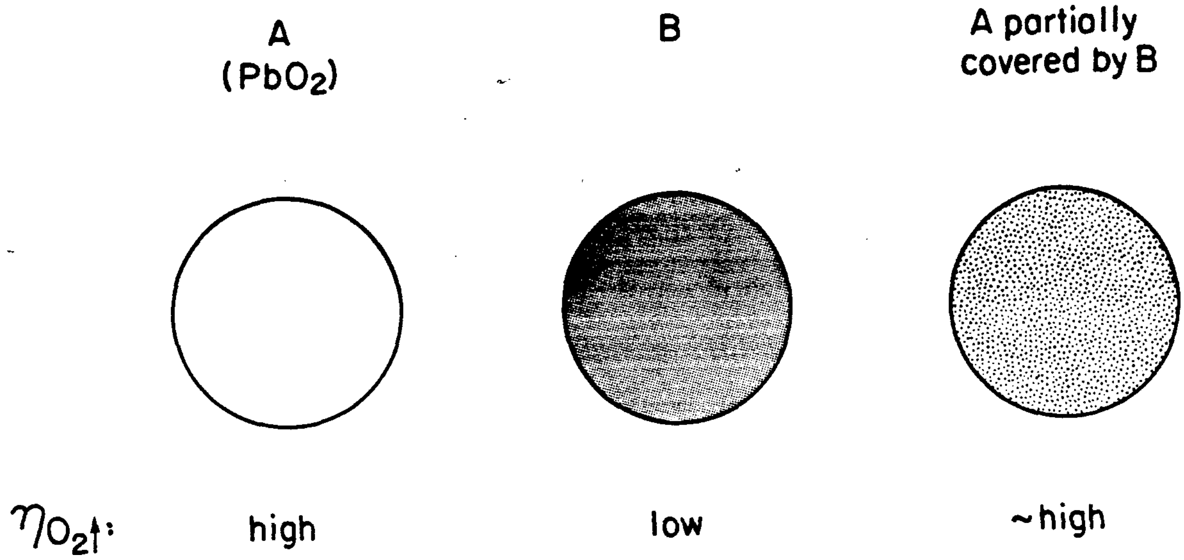

Figure 2. Schematic illustration for the strategy to modify PbO_2 electrode for selective electrocatalysis of oxygen-transfer reactions

Region: (A) inert electrode material with high oxygen-evolution overpotential,
(B) active electrode material with low oxygen-evolution overpotential

II. KINETICS AND MECHANISM OF ELECTRODEPOSITION OF LEAD DIOXIDE IN ACIDIC MEDIA

A. Chronoamperometric and Voltammetric Studies of the Nucleation and Electrodeposition of ß-Lead Dioxide at a Rotated Gold Disc Electrode[1]

"If it is possible to cut out a word, then always cut it out."

-George Orwell,
"Politics and the English Language"

---

[1] Published in Chang, H.; Johnson, D. C. J. Electrochem. Soc. 1989, 136, 17-22.

Abstract

The electrodeposition of ß-PbO_2 from $HClO_4$ solutions of Pb(II) at a Au rotated disc electrode (RDE) was studied as a function of applied potential, rotational velocity, and the concentrations of $HClO_4$ and Pb(II). A long induction period (i.e., $i \simeq 0$) is associated with high acidity, low concentration of Pb(II), and high rotational velocity. Following the induction period, the current rises to a steady-state value which is significantly lower than the mass transport-limited value for Pb(II). The steady-state value of electrode current decreases as rotational velocity is increased, contrary to expectations for a mass transport-controlled process at a RDE. The generation of a soluble intermediate species is proposed to account for these observations.

Repeated cycles of deposition and stripping of PbO_2 at the Au RDE results in a decreasing induction period for subsequent PbO_2 deposition. This is concluded to result because an ultra-thin Pb(II) film (possibly PbO) is formed which is stabilized by interaction with the Au substrate and is not dissolved following the negative potential scan to 0.3 V. The original state of the clean Au surface is regenerated by cathodic $H_2(g)$ evolution, chemical stripping with H_2O_2 or $KMnO_4$, or by mechanical abrasion.

Introduction

Recently in this laboratory, pure and extensively doped ß-PbO_2 electrodes have been studied for their electrocatalytic properties in support of anodic oxidation reactions involving simultaneous transfer of oxygen from the H_2O solvent to the reaction products (1). These oxide materials are electrochemically deposited onto Au or Pt rotated disc electrodes (RDEs) in acidic media ($pH < 1$). This work is part of a general search for unique anode materials with catalytic properties surpassing those of the more traditional anodes (i.e., C, Pt and Au) for use as amperometric transducers. Significance is projected also for larger-scale industrial processes. Lead dioxide was chosen as the host oxide in these experiments because of its relatively high electrical conductivity, low cost, ease of preparation, inertness in both acidic and alkaline solutions, and stability at high temperatures. Furthermore, this oxide is not a stoichiometric dioxide (i.e., PbO_x, $1.9 < x < 2.0$) (2) and it was suspected that defect sites might exist on the electrode surface which can participate catalytically in anodic O-transfer reactions.

Pure electrodeposited ß-PbO_2 was demonstrated to exhibit a moderate electrocatalytic activity for supporting various anodic reactions in acidic media, especially for sulfur compounds. However, that activity can be increased greatly for numerous reactions by incorporation of group VA metals, especially bismuth, to form the mixed oxides (1b-e). Since the anodic electrodeposition of PbO_2 from aqueous solutions of Pb(II) requires oxygen transfer, a clearer understanding of the deposition mechanism could provide valuable insight into the mechanisms of anodic O-transfer reactions at the pure and mixed-oxide electrodes.

An intense interest in the PbO_2-Pb(II) redox couple has existed because of the use of PbO_2 in lead-acid batteries (2,3), as well as for anodes in electrosynthesis (4). Secondary interest in the redox couple has resulted because the deposition of PbO_2 is a unique model for testing electrocrystallization theories (5,6). Summaries of the literature are cited (7). Most published studies of PbO_2 have focused on physical properties (morphology, density, porosity, durability, and surface area) of the oxide deposited at high current densities and pH 3 - 7, and the discharge/recharge kinetics in H_2SO_4 media. Little work has been concerned with kinetics and mechanisms in acidic media other than H_2SO_4. The anodic reaction has served also for preconcentration of Pb(II) in the electrogravimetric (8) and cathodic stripping determinations of trace levels of the metal ion in water (9).

Fleischman et al. (5) were the first to consider in depth the complexity of the mechanism for electrodeposition of PbO_2 from aqueous solutions of Pb(II). Their mechanism, summarized by [1-4], has received wide support (4a,9b,10).

$$OH^- \Longleftrightarrow OH_{ads} + e \qquad [1]$$

$$Pb^{2+} + (OH)_{ads} + OH^- \longrightarrow Pb(OH)^{+}{}_{2,ads} \qquad \text{(slow)} \qquad [2]$$

$$Pb^{2+} + (OH)_{ads} + OH^- \longrightarrow Pb(OH)^{2+}{}_{2,ads} + e \qquad \text{(slow)} \qquad [3]$$

$$Pb(OH)^{2+}{}_{2,ads} \Longleftrightarrow PbO_2(s) + 2H^+ \qquad [4]$$

Alternately, the production of $Pb(OH)^{2+}{}_{2,ads}$ in [3] can be written based on the oxidation of $Pb(OH)^{+}{}_{2,ads}$ from [2]. The products of [2] and [3] were postulated to be insoluble and adsorbed on the substrate.

The majority of studies of PbO_2 electrodeposition have been performed in unstirred solutions, with only a few at hydrodynamic electrodes (9b,11). Application of the rotated disc electrode (RDE) is appropriate for mechanistic studies of multi-electron processes with coupled chemical reactions because of the large dynamic range for mass transfer available at this electrode. Here we describe chronoamperometric and voltammetric data for a Au RDE as a function of rotational velocity, deposition potential, and the concentrations of $HClO_4$ and Pb(II). We propose that a significant solubility exists for the intermediate products of the PbO_2 deposition process.

Experimental

Reagents Chemicals were Reagent Grade and water was distilled followed by purification in a Barnstead NANOpure-II system (Boston, MA). Lead(II) solutions were prepared by dissolution of PbO in $HClO_4$. In studies of the effect of $HClO_4$ concentration, $NaClO_4$ was added to maintain constant ionic strength. The Cl^- impurity in all solutions was $< 1\ \mu M$, as calculated from impurity levels specified on the reagent bottles.

Instrumentation Disc electrodes were constructed from gold (44.7 mm^2), platinum (45.6 mm^2) and glassy carbon (19.1 mm^2) by Pine Instrument Co. (Grove City, PA). A PIR rotator and RDE4 potentiostat (Pine Instrument Co.) also were used. Electrode potentials were controlled vs. a saturated calomel electrode (SCE; Fischer Scientific, Inc.) contacting the electrolysis solution through a Luggin capillary. The Pt-wire counter electrode was located in a separate chamber filled with the supporting electrolyte and contacting the electrolysis solution through a fritted glass membrane.

Procedures Disc electrodes were polished prior to every experiment with 0.05-µm alumina on microcloth (Buehler, Ltd.), except as noted. Solid PbO_2 deposits were removed electrolytically at 0.2 V, prior to removal of the RDE from the electrolysis solution, followed by chemical stripping of any oxide residue in a 1:1 mixture of acetic acid and hydrogen peroxide (30%). Amperometric data were obtained in triplicate and average values are reported.

Results and discussions

Analysis of transient current-time curves A typical chronoamperometric response (i-t) for PbO_2 deposition at the Au RDE in $HClO_4$ solution is shown in Figure 1. Recording of the i-t curve was started for the freshly polished RDE immediately following the first potential step from 0.2 V to 1.6 V. The transient curve shown is divided into four regions to facilitate discussion. The induction period (A), with a time period t_o, corresponds to a relatively small electrode current ($i \simeq 0$). Previous designations of t_o have been based on the first apparent departure of current from zero (4a,5,6). That is a rather arbitrary and subjective definition depending on the current sensitivity of the recorder. Our designation of t_o is applied easily. The value of t_o shown in Figure 1 is significantly longer than reported previously (4a,5a-b) for pH 2 - 5. This will be demonstrated to be the consequence of rotation of the RDE and lower pH.

Region B (Figure 1), with a time period designated t_1, corresponds to rapid growth of PbO_2 nuclei with a corresponding transition of the electrode current from virtually zero to a steady-state value (i_{ss}). Historically, it is the early part of Region B (i.e., $0 < i \ll i_{ss}$) which has received the greatest attention in electrocrystallization studies (4a,5a,6,9-12). For two dimensional growth, which is assumed for the initial monolayer of oxide, the value of i is predicted to be proportional to $(t-t_o)^2$, whereas for three-dimensional growth, i.e., bulk deposition, i is predicted to be proportional to $(t-t_o)^3$ (12). However, for $t-t_o \simeq 0$, it is difficult to discern between the second and third order dependencies, and a clear transition from two-dimensional to three-dimensional growth kinetics is difficult to determine. We shall use the value of t_1 and the estimated slope (S) of the i-t curve at $i = 0.5i_{ss}$ (i.e., $S = i_{ss}/t_1$) to characterize Region B.

Region C (Figure 2-1) corresponds to the observation of a steady-state value of electrode current (i_{ss}). The steady-state current has been proposed to be the mass-transport limited value (10); however, this clearly is not the case here. For $C^b_{Pb(II)} = 0.2$ M, the transport-limited steady-state current would be much in excess of values shown in Figure 1. Hence, the reaction is concluded to be under kinetic control.

Results of a typical study of the steady-state current as a function of rotational velocity (w) are shown as Region D of Figure 1. For a mass-transport limited, steady-state reaction, values of i_{ss} are expected to increase proportionally to $w^{1/2}$. Hence, the decrease of i_{ss} with increasing $w^{1/2}$ is concluded to be a significant indicator of the mechanistic complexity of the deposition reaction. Observations in Region D are discussed further in a later section.

Variation of Pb(II) and $HClO_4$ concentrations The dependence of t_o, t_1, S, and i_{ss} on $C^b_{Pb(II)}$ was studied for 1.70 M $HClO_4$ at a rotation speed of 0 rev min^{-1}. Clearly, t_o decreased with increasing $C^b_{Pb(II)}$, which is in agreement with the mechanism of [1-4]. The value of i_{ss} increased as a linear function of $C^b_{Pb(II)}$, which also is consistent with the pseudo-first order dependence of the deposition rate on $C^b_{Pb(II)}$ for the mechanism under consideration. It should be noted that for 0 rev min^{-1}, a steady-state current was observed. This value of i_{ss} was much lower than the diffusion-limited current, i.e., the Cottrell current, which is, along with the observed absence of a time dependence in Region C, further evidence for the designation of total control of electrode current by the deposition kinetics. Hence, there is virtually no concentration polarization, and $C^s_{Pb(II)} \simeq C^b_{Pb(II)}$. The value of S increased with increasing $C^b_{Pb(II)}$ both because of the increase in i_{ss} and the decrease in t_1.

The dependence of t_o, t_1, S and i_{ss} on C^b_{HClO4} also was studied at 0 rev min^{-1}. Values of i_{ss} and S decreased substantially, and t_o and t_1 increased, as C^b_{HClO4} was increased (pH decreased). This is consistent with the mechanism in [1-4], since higher H^+ concentration should decrease the equilibrium surface activity of OH_{ads} in [1] for a constant electrode potential. However, the dependencies could not be linearized by resorting to customary plotting strategies, i.e., log-log, etc. Hence, estimation of reaction order was not possible.

Variation of rotational velocity   Changes in t_o, t_1 and S with increasing values of $w^{1/2}$ are shown in Figure 2. The positive linear t_o-$w^{1/2}$ dependence is concluded to be the result of the solubility of one or both of the intermediate products of the induction period proposed in [2,3], i.e., $Pb(OH)_2{}^+$ and/or $Pb(OH)_2{}^{2+}$. These soluble intermediate products are transported away from the electrode, by the convective-diffusion mechanism, and nucleation as well as growth of existing nuclei is defeated in [4]. The decrease in S shown in Figure 2 is a result largely of the decrease in i_{ss} with increased $w^{1/2}$.

Further study of the dependence of i_{ss} on $w^{1/2}$ was made using two strategies. Method A: The value of $w^{1/2}$ desired for the measurement of i_{ss} in Period C - D was used also for Periods A and B. According to the standard procedure, the electrode surface was also cathodically stripped and mechanically polished preliminary to the application of each new value of w. Method B: A single low value of w was used for Periods A and B, and then the measurement of i_{ss} vs. w was performed in Periods C - D exactly as shown in Figure 1. This procedure was very rapid in comparison to Method A. Values of current from the two methods ($i_{ss,A}$ and $i_{ss,B}$) are shown in Figure 3. For fixed values of C^b_{HClO4} and $w^{1/2}$, i_{ss} increases with increasing $C^b_{Pb(II)}$, which is consistent with results of the study of $C^b_{Pb(II)}$ dependence. From Figure 3 it can be seen that $i_{ss,A}$ and $i_{ss,B}$ are very similar, provided that other conditions are the same. Whereas some increase in i_{ss} was seen for a slight increase of w above 0 rev min^{-1} (Figure 3), generally the increase in $w^{1/2} > 20$ (rev $min^{-1})^{1/2}$ resulted in no change of $i_{ss,A,B}$ values for small C^b_{HClO4}.

However, a definite inverse dependence on $w^{1/2}$ was observed for large values of C^b_{HClO4} and $C^b_{Pb(II)}$. A similar phenomenon has been described briefly using electrogravimetry for a rotated Pt gauze electrode (8). However, the extent of the study apparently was limited and a detailed mechanistic interpretation of the observation was not offered. The decrease in i_{ss} for increasing $w^{1/2}$ is consistent with the conclusion of the finite solubility of the intermediate products during Periods C - D. We conclude the soluble products are generated throughout Regions A - D.

To minimize the number of figures showing i_{ss}-$w^{1/2}$ plots, the dependencies of the i_{ss}-$w^{1/2}$ relationship on $C^b_{Pb(II)}$ and C^b_{HClO4} are summarized further in Figure 4 for $E_{dep} = 1.48$ V. Three distinct regions denoting the different characteristics of the deposition kinetics can be designated on the $C^b_{Pb(II)}$-C^b_{HClO4} plane. A linear dependence of i_{ss} on $w^{1/2}$ characteristic of a transport-limited process was observed only in Region A (Figure 4). The value of i_{ss} decreases linearly with increasing $w^{1/2}$ in Region B (Figure 4). For the boundary region between A and B, the i_{ss}-$w^{1/2}$ dependence is irregular. For example, with $C^b_{Pb(II)} = 0.05$ M and $C^b_{HClO4} = 0.4$ M, i_{ss} increases with $w^{1/2}$ at low w values but decreases at higher $w^{1/2}$ values. This result is consistent with the conclusion of mixed kinetics-transport control.

Variation of deposition potential   The dependencies of t_o, t_1, S and i_{ss} on E_{dep} are shown in Figure 5. These results are similar to others which are not shown which were obtained as a function of $C^b{}_{Pb(II)}$ and $C^b{}_{HClO4}$. The values of t_o and t_1 decrease and values of S and i_{ss} increase with increasing E_{dep}. The primary influence of E_{dep} on the deposition kinetics is expected to come by way of [1] which controls the surface activity of OH_{ads} in [2]. The tendency for i_{ss} values to decrease with increasing $w^{1/2}$ was observed for all values E_{dep} = 1.440 - 1.560 V. For the values of E_{dep} used to obtain data in Figures 1 - 5, the contribution of O_2 production to i_{ss} was negligible.

Correlation between PbO_2 deposition and O_2 evolution It is noted that the initial step [1] in the PbO_2 deposition mechanism is also the first step for the anodic evolution of O_2 at most metal-oxide electrodes (12). It has been proposed also that this is the first step in anodic surface-catalyzed O-transfer reactions (5). It was expected, therefore, that a perceptible rate of nucleation and deposition of PbO_2 on the Au RDE, as well as for Pt and GC, might be observed only when there is a small simultaneous anodic generation of O_2. This is proved to be the case by the voltammetric data in Figure 6. The activation overpotential for O_2 evolution (η) is significantly different for Au, Pt and GC ($\eta_{GC} > \eta_{Au} > \eta_{Pt}$). Hence, the minimum potential value appropriate to initiate an observable rate of PbO_2 deposition is different for the three materials ($E_{dep,GC} > E_{dep,Au} > E_{dep,Pt}$).

The observed differences in O_2-evolution potential became negligible for the three substrates when their respective surfaces were covered with PbO_2. Hence, for the negative potential scans in Figure 6, the apparent half-wave potential values are approximately the same for each curve. When the substrate of any individual electrode becomes covered with PbO_2, continued deposition of PbO_2 occurs only if E_{dep} is appropriate for an appreciable rate of O_2 evolution on the PbO_2 deposit. Consequently for

Pt, since η_{Pt} is slightly less than for η_{PbO2}, the minimal potential required to initiate PbO_2 deposition on Pt is slightly less than is sufficient to maintain a significant rate of continued PbO_2 growth.

The relationship between O_2 evolution and PbO_2 deposition was studied further by constant-potential chronoamperometry. The induction time (t_o) was determined as a function of E_{dep} for the different electrodes. The value of t_o was determined to be approximately inversely related to the residual current for O_2 evolution observed at that value of E_{dep}. Since the O_2 evolution rate is an exponential function of potential, the plot of log t_o vs. E_{dep} was expected to be linear. Furthermore, for any given value of E_{dep} for the three electrodes, it was expected that $t_{o,GC} > t_{o,Au} > t_{o,Pt}$ since $\eta_{GC} > \eta_{Au} > \eta_{Pt}$. A plot of log t_o vs. E_{dep} is shown in Figure 7. We propose that the induction time (t_o) is inversely related to the nucleation rate at the clean electrode surfaces and, therefore, the plot of log t_o vs. E_{dep} corresponds to a Tafel plot for the deposition process. The slopes of these plots are approximately equivalent; however, the differences in intercept are large and are consistent with the difference in η for O_2 evolution at the three electrode materials. A linear plot of log t_o vs. E_{dep} also was presented by Ramamurthy and Kuwana (4a), but without explanation.

Effects of added foreign anions The rate of electrodeposition of ß-PbO_2 is maximized, in general, by use of small w, low C^b_{HClO4} and large $C^b_{Pb(II)}$. The effect of added inert anions also was considered. Results show that co-existing NO_3^- and ClO_4^- of varied concentration and small amounts of SO_4^{2-}, held to less than 10^{-5} M to prevent precipitation of

$PbSO_4(s)$, do not have a significant effect on t_o. However, NO_3^- tends to increase and ClO_4^- slightly decreases the value of i_{ss}. It had been shown (1e) that if the SO_4^{2-} concentration is comparable to $C^b_{Pb(II)}$, t_o is shortened significantly and i_{ss} is increased. Since the standard potential of the PbO_2-$PbSO_4$ couple (1.69 V) is higher than that of the PbO_2-Pb(II) couple (1.47 V) (13), it does not appear likely that this effect can be explained well by the stabilization by SO_4^{2-} of soluble intermediates generated during the nucleation process. It was determined that addition of Cl^- impurity to ca. 10 M did not change the results reported here. The influence of high levels of Cl^- (> 100 μM) is under study.

Effects of voltammetric electrode pretreatment Multiple cyclic scans of applied potential at noble metal electrodes have been demonstrated to cause enhancement of some electrode reactions, especially when the potential scans result in the alternate anodic/cathodic formation/dissolution of surface oxide. The observed effect has been attributed to the benefits of oxide-catalyzed oxidative removal of adsorbed impurities (1b), as well as to the increase of surface area by way of surface reconstruction (14).

The alternate anodic deposition and cathodic stripping of PbO_2 at Au and Pt RDEs was observed to decrease substantially the induction period (t_o) for the subsequent deposition. The phenomenon is demonstrated by changes in voltammetric response (i-E) shown in Figure 8 as a function of scan number. The rate of anodic PbO_2 deposition at E_{dep} > ca. 1.5 V increases significantly with scan number for cyclic scans between the limits 0.3 V and 1.8 V. The anodic current (i_a) at 1.8 V is shown plotted vs. scan number in the figure inset. The cathodic peak ($i_{p,c}$) for stripping of PbO_2 on the negative scan at ca. 1.2 V increases in height and area with scan number, as expected when larger quantities of PbO_2 are deposited in the region 1.55 - 1.80 V due to the decrease of t_o with increasing cycle number. The cathodic peak at ca. 0.9 V corresponds to the reduction of gold oxide formed for E > ca. 1.0 V and remains relatively unchanged with cycle number.

On the basis of Figure 8, it is concluded that the increases in i_a and $i_{p,c}$ are the direct result of an increased number of nucleation sites at the electrode surface. This increase cannot possibly be explained as the result of surface reconstruction (roughening) which might occur with repeated formation/dissolution of gold oxide because the area of the peak for gold oxide reduction remained unchanged. Furthermore, numerous cyclic scans between 0.3 V and 1.8 V prior to addition of Pb(II) to the electrolyte failed to produce the enhancement of deposition rates demonstrated in Figure 8. The return of i-E response from that for the 10th scan to that for the first scan in Figure 8 was achieved by any of the following processes: mechanical abrasion (0.05 µm alumina), chemical treatment with H_2O_2 or $KMnO_4$, or cathodic evolution of $H_2(g)$ at $E << -0.3$ V. It is concluded that an ultra-thin film of adsorbed Pb(II) is formed by the plating/stripping process and the adsorbed metal ions are rapidly oxidized to adsorbed PbO_2 which serve as nucleation sites for the subsequent deposition of bulk $PbO_2(s)$. The fractional surface coverage by adsorbed Pb(II) increases with cycle number and becomes constant only when a complete film is formed (e.g., cycle number > 9). The presence of an adsorbed lead species on the Au surface following the voltammetric stripping of $PbO_2(s)$ at 0.3 V was verified by X-ray photoelectron spectroscopy (XPS).

The peak areas in Figure 8 corresponding to the cathodic and anodic current were measured by the "cut-and-weigh" method. It was found that the stripping peak area was virtually the same (ca. 0.1%) as the anodic area and we conclude that all Pb(IV) formed during the anodic process is converted to Pb(II) during cathodic stripping. Therefore the adsorbed lead species cannot be Pb(IV). Following the experiment shown in Figure 8, the Au electrode was rinsed and put in a 1.0 M $HClO_4$ blank solution and the potential was scanned from 1.3 to 1.8 and back to 1.3 V. A small but distinct PbO_2 deposition peak was observed which corresponded to the oxidation of the ultra-thin Pb(II) film at the anodic region. Hence, it can be concluded from Figure 8 that the number of nucleation sites increases with each cycle of $PbO_2(s)$ deposition/stripping. Chemical (H_2O_2 and $KMnO_4$) and electrochemical (H_2 evolution) removal of residual nucleation sites is very efficient. Although the ultra-thin film is stable in the region $1.1 > E > 0.3$ V, there was no evidence for underpotential deposition of lead at a clean Au surface during the positive scan for $0.3 < E < 1.1$ V.

The effect of the ultra-thin Pb(II) film on PbO_2 deposition also is demonstrated by the chronoamperometric curves shown in Figure 9. After the formation of a substantial deposit of PbO_2 at 1.48 V, the PbO_2 was stripped cathodically at 0.3 V. Then, PbO_2 was redeposited at 1.48 V without further treatment of the electrode surface. From the redeposition current, it can be seen that t_o has decreased nearly to zero and i_{ss} for deposition of PbO_2 is achieved quickly.

The effect of variation of C^b_{HClO4} on the first (A) and reproducible (B) i-E curves is shown in Figure 10 for potential scans in the range 0.3 - 1.8 V. As C^b_{HClO4} is decreased, the anodic current at 1.7 V and anodic area of the wave for $E > 1.5$ V increases and, correspondingly, the height and area of the cathodic stripping peak in the region 1.3 - 1.1 V are increased. It is concluded that the number of nucleation sites generated on the first scan is inversely related to C^b_{HClO4}. Both the area and height of the deposition wave and stripping peak for curve d in Figures 10A & B (0.40 M $HClO_4$) change only slightly with cycle number. This is because for this pH, the entire surface of Au is covered by the ultra-thin Pb(II) film after a single cycle of deposition and stripping. These observations and conclusions are consistent with chronoamperometric data in Figures 2 - 5. For the reproducible i-E curve (Figure 10B), the anodic current at 1.7 - 1.8 V is relatively independent of C^b_{HClO4}, as compared to the first scan (Figure 10A). Hence, the maximum number of nuclei which can be formed apparently is relatively independent of C^b_{HClO4}. The shift of peak potential for the stripping process with change in pH (Figures 10A&B) indicates involvement of H^+ in the stripping process.

Optimization of electrodeposition conditions One purpose of this research was the determination of optimal conditions for PbO_2 deposition. Based on the results of the kinetic and mechanistic studies of PbO_2

deposition at varied conditions as shown above, the following optimal conditions were chosen: 20 mM Pb(II), 0.1 M $HClO_4$, 400 rev min^{-1}, and an initial value $E_{dep} = 1.6$ V vs. SCE. When the current has reached its maximum value, e.g., ca. 5 sec, E_{dep} is decreased to 1.5 V for the remaining deposition period of 60 - 90 sec. The PbO_2 film prepared in this way is smooth, very adhesive,. and highly reflective.

Conclusions

The mechanism of PbO_2 electrodeposition is concluded to involve the generation of a soluble intermediate product which can be transported away from the electrode surface by convective-diffusional processes. Hence, solution agitation can result in a significant barrier for deposition.

When $C^b_{Pb(II)}$ and C^b_{HC104} are large, deposition is under kinetic control and the rate of deposition decreases with increased rotation rate. Furthermore, the steady-state current for deposition is much less than the mass-transport limited value. The reaction is under mass-transport control only when both $C^b_{Pb(II)}$ and C^b_{HC104} are low. In this case, the rate of deposition increases with increased rotational velocity. For medium values of $C^b_{Pb(II)}$ and C^b_{HC104}, the deposition is under mixed control by kinetics and mass-transport. The rate of deposition is relatively independent of rotation rate at the RDE.

It is observed that, in general, the electrodeposition of PbO_2 on Au, Pt, GC, and on PbO_2 itself, occurs at a significant rate only for potential values corresponding to a finite rate for the simultaneous evolution of O_2. The mechanism of O_2 evolution (12d) on oxides is proposed to correspond to the rapid initial reaction

$$H_2O \longrightarrow OH_{ads} + H^+ + e \quad \text{(fast)} \qquad [5]$$

Hence, the OH_{ads} generated by the O_2-evolution reaction [5] can be consumed within the PbO_2 deposition mechanism, as shown in [2]. The rate of O_2 evolution for low anodic current densities at oxide-covered Pt, Au and Pb anodes increases with increase in pH by the amount 0.0591 pH and as an exponential function of applied potential (12d). Accordingly, it is observed that the rate of PbO_2 deposition increases as the values of pH and E_{dep} are increased.

Formation and stripping of PbO_2 during potential cycling produces an electrode surface bearing an ultra-thin film of a Pb(II). This ultra-thin film is stable to 0.3 V vs. SCE, but can be stripped from the electrode by cathodic evolution of H_2 or chemical treatment with H_2O_2 or $KMnO_4$. The ultra-thin Pb(II) film is rapidly oxidized to PbO_2 at $E > 1.3$ V and serves to nucleate the further deposition of bulk $PbO_2(s)$. Further studies of the mechanism of ultra-thin film formation will be published elsewhere.

References

1. (a) Austin, D. S.; Polta, J. A.; Polta, T. Z.; Tang, A. P.-C.; Cabelka, T. P.; Johnson, D. C. J. Electroanal. Chem. 1984, 168, 227. (b) Johnson, D. C.; Polta, J. A.; Polta, T. Z.; Neuburger, G. G.; Johnson, J.; Tang, A. P.-C.; Yeo, I.-H.; Baur, J. J. Chem. Soc., Faraday Trans. 1 1986, 82, 1081. (c) Tang, A. P.-C.; Johnson, D. C. Anal. Chim. Acta in press. (d) Yeo, I.-H.; Johnson, D. C. J. Electrochem. Soc. 1987, 134, 1973. (e) Yeo, I.-H. Ph.D. Dissertation, Iowa State University, Ames, Iowa, 1987. (f) Wels, B.; Johnson, D. C. not published.

2. Carr, J. P.; Hampson, N. A. Chem. Rev. 1972, 72, 679.

3. (a) Lazarides, C.; Hampson, N. A.; Henderson, M. J. Appl. Electrochem. 1981, 11, 605. (b) "Batteries"; Vol. 2, Kordesch, K. V., Ed.; M. Dekker: New York, 1977.

4. (a) Ramamurthy, A. C.; Kuwana, T. J. Electroanal. Chem. 1982, 135, 243. (b) Narasimham, K. C.; Gomathi, P. S.; Udupa, H. V. K. J. Appl. Electrochem. 1976, 6, 397. (c) Gnanasekaran, K. S. A.; Narasimham, K. C.; Udupa, H. V. K. J. Appl. Electrochem. 1976, 6, 189. (d) Hampel, C. A. "The Encyclopedia of Electrochemistry"; Chapman and Hall: London, 1964; p. 762.

5. (a) Fleischmann, M.; Liler, M. Trans. Faraday Soc. 1958, 54, 1370. (b) Fleischmann, M.; Thirsk, H. R. Electrochim. Acta 1959, 1, 146. (c) Fleischmann, M.; Thirsk, H. R. Electrochim. Acta 1960, 2, 22. (d) Fleischmann, M.; Mansfield, J. R.; Thirsk, H. K.; Wilson, H. G. E.; Wynne-Jones, L. Electrochim. Acta 1967, 12, 967.

6. (a) Barradas, R. G.; Contractor, A. Q. J. Electroanal. Chem. 1982, 138, 425. (b) Barradas, R. G.; Contractor, A. Q. J. Electroanal. Chem. 1981, 129, 327. (c) Stevens, R.; Gilroy, D. J. Microscopy 1981, 124, 265. (d) Gilroy, D.; Stevens, R. J. App. Electrochem. 1980, 10, 51.

7. (a) "The Electrochemistry of Lead"; Kuhn, A. T., Ed.; Academic Press: London, 1979. (b) Pohl, J. P.; Richert, H. In "Electrodes of Conductive Metallic Oxides"; Trasatti, S., Ed.; Elsevier: Amsterdam, 1980. (c) Nagy, Z. "Electrochemical Synthesis of Inorganic Compounds: A Bibliography"; Plenum Press: New York, 1985.

8. (a) Nichols, M. L. Ind. Eng. Chem., Anal. Ed. 1931, 3, 384. (b) Day, T. G.; Delano, P. H.; Schrenk, W. T. Bulletin-Missouri School of Mines and Metallurgy, U. Missouri-Rolla, 1935, 12, No. 1, 1. (c) Lingane, J. J. "Electroanalytical Chemistry"; 2nd edition, Interscience: New York, 1958; p. 374

9. (a) Laitinen, H. A.; Watkins, N. H. Anal. Chem. 1975, 47, 1352. (b) Laitinen, H. A.; Watkins, N. H. J. Electrochem. Soc. 1976, 123, 804. (c) Kinard, J. T.; Propst, R. C. Anal. Chem. 1974, 46, 1106.

10. (a) Beck, F. J. Electroanal Chem. 1975, 65, 231. (b) Beck, F.; Boh, H. Ber. Bunsenges. Phys. Chem. 1975, 79, 233. (c) Hampson, N. A.; Jones, P. C.; Phillips, R. F. Can. J. Chem. 1968, 46, 1325. (d) Hampson, N. A.; Jones, P. C.; Phillips, R. F. Can. J. Chem. 1967, 45, 2039. (e) Hampson, N. A.; Jones, P. C.; Phillips, R. F. Can. J. Chem. 1967, 45, 2045.

11. Nishibe, K. Denki Kagaku 1984, 52, 614; Chem. Abstr. 102, 13988c.

12. (a) Fleischmann, M.; Thirsk, H. R. In "Advances in Electrochemistry and Electrochemical Engineering"; Delahay, P.; Tobias, C. W., Eds.; Interscience: New York, 1963; Volume 3; *J. Electrochem. Soc., Japan (overseas suppl. ed.)* 1960, 28, E175. (b) Dignam, M. J. In "Comprehensive Treatise of Electrochemistry"; Bockris, J. O'M.; Conway, B. E.; Yeager, E.; White, R. E., Eds.; Plenum Press: New York, 1981; Volume 4. (c) Greef, R.; Peat, R.; Peter, L. M.; Pletcher, D.; Robinson, J. "Instrumental Methods in Electrochemistry"; Ellis Horwood: Chichester, 1985; Chapter 9. (d) Tarasevich, M. R.; Sadkowski, A.; Yeager, E. In "Comprehensive Treatise of Electrochemistry," Conway, B. E.; Bockris, J. O'M.; Yeager, E.; Khan, S. U. M.; White, R. E., Eds.; Plenum Press: New York, 1983; Volumne 7.

13. "Standard Potentials in Aqueous Solutions"; Bard, A. J.; Parsons, R.; Jordan, J., Eds.; Marcel Dekker: New York, 1985; p. 220.

14. (a) Chialvo, A. C.; Triaca, W. E.; Arvia, A. J. *J. Electroanal. Chem.* 1983, 146, 93. (b) Chialvo, A. C.; Triaca, W. E.; Arvia, A. J. *J. Electroanal. Chem.* 1984, 171, 303. (c) Herman, E. G.; Alonso, C.; Gonzalez-Velasco, J. *J. Electroanal. Chem.* 1987, 233, 277. (d) Kinoshita, K. In "Modern Aspects in Electrochemistry"; Bockris, J. O'M.; Conway, B. E.; White, R. E., Eds.; Plenum Press: New York, 1982; Volume 14. (e) Kinoshita, K.; Lundquist, J. T.; Stonehart, P. *J. Electroanal. Chem.* 1973, 48, 157. (f) Bishop, E.; Hitchcock, P. H. *Analyst* 1973, 98, 475.

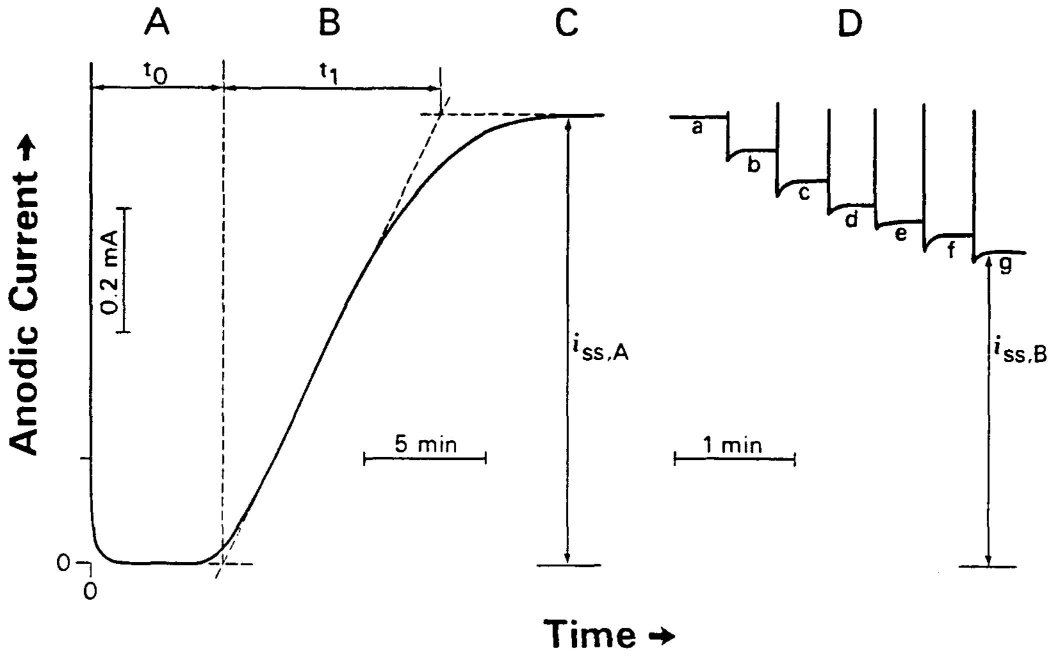

Figure 1. A typical chronomamperometric transient (i-t) for PbO_2 deposition at a Au RDE

Conditions: 0.20 M Pb(II), and 1.70 M $HClO_4$

Regions:
(A) induction period (t_o),
(B) transition period (t_1),
(C) steady-state period ($t \gg t_o + t_1$),
(D) study of rotation speed dependence on i_{ss}

Rotation velocity (rev min^{-1}): (a) 0, (b) 400, (c) 900, (d) 1600, (e) 2500, (f) 3600, and (g) 4900

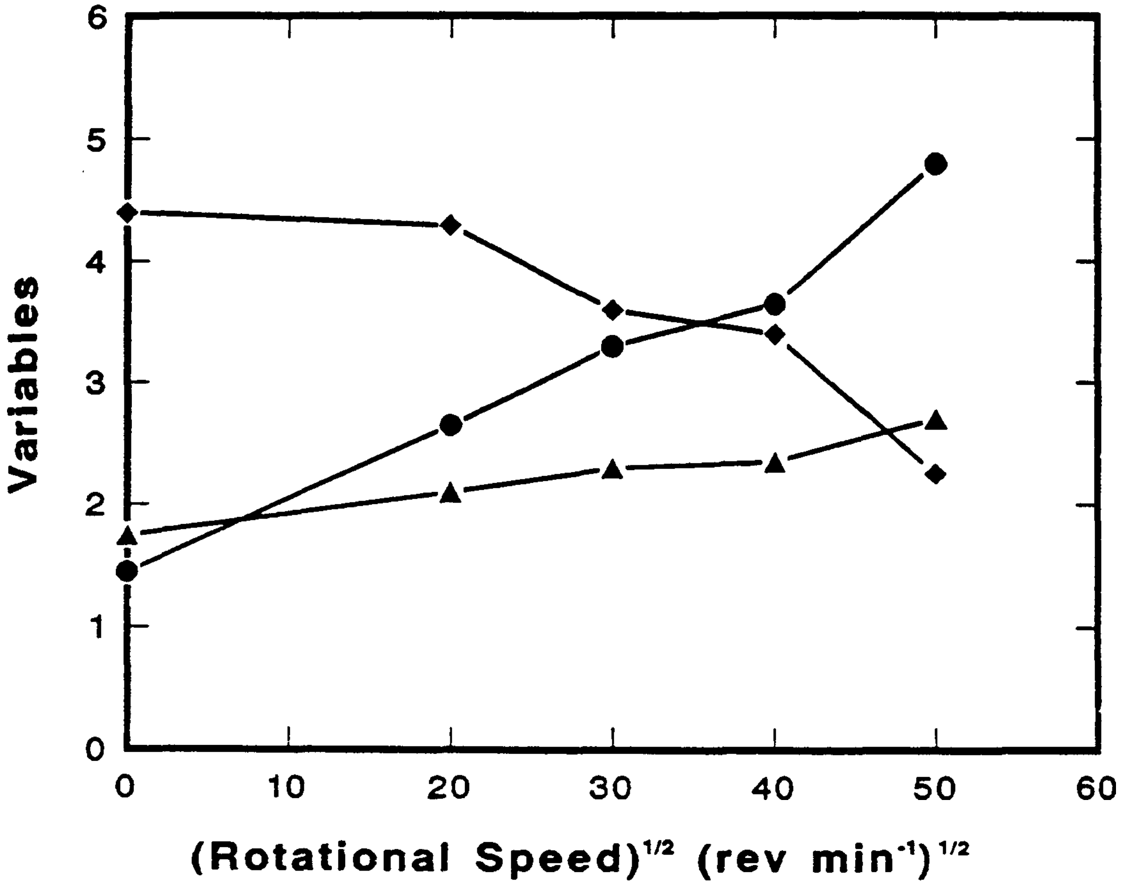

Figure 2. Plots of t_o, t_1, and S vs. $w^{1/2}$

Conditions: 0.20 M Pb(II), 1.30 M $HClO_4$, and 0.40 M $NaClO_4$

Variables: (●) t_o/min, (▲) t_1/min, (◆) S/0.1 mA min^{-1}

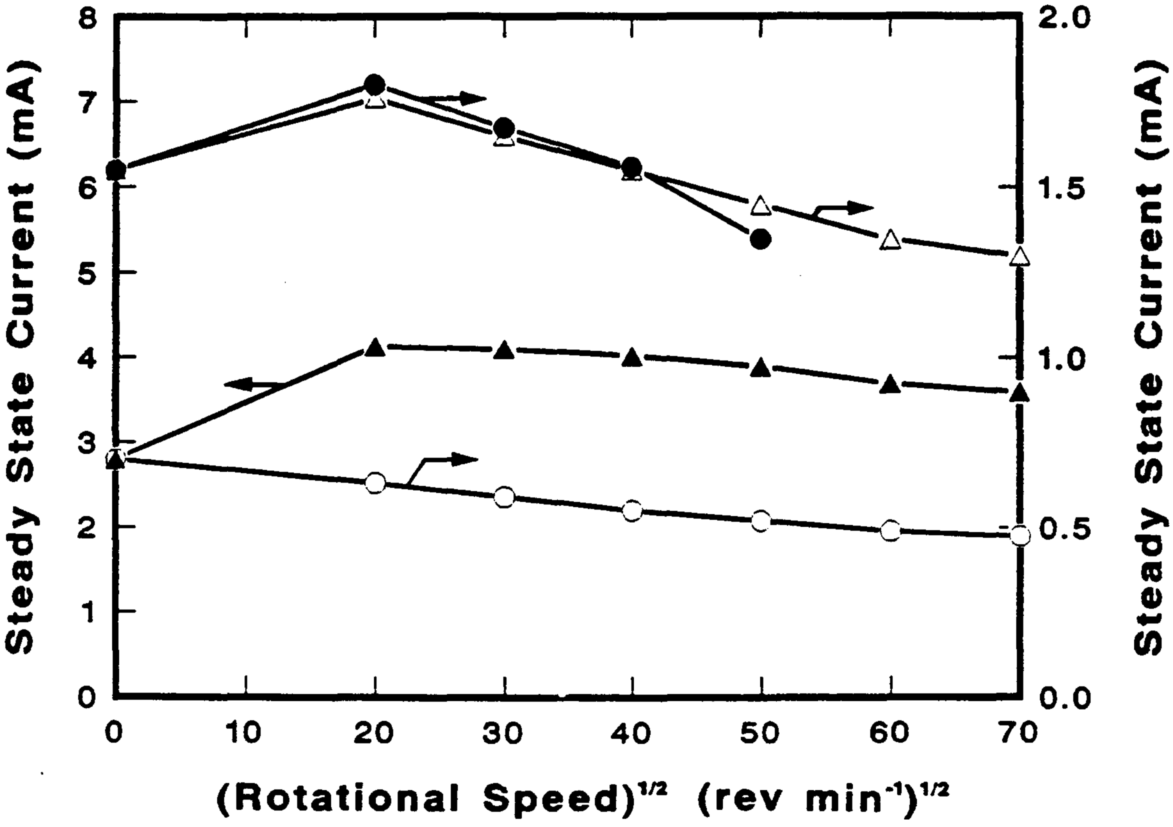

Figure 3. Plots of i_{ss} vs. $w^{1/2}$ as a function of C^{b}_{HClO4}

Conditions: 0.20 M Pb(II)

Variable and C^{b}_{HClO4}: (●) $i_{ss,A}$ for 1.30 M,
(▲) $i_{ss,A}$ for 0.80 M,
(○) $i_{ss,B}$ for 1.70 M,
(△) $i_{ss,B}$ for 1.30 M

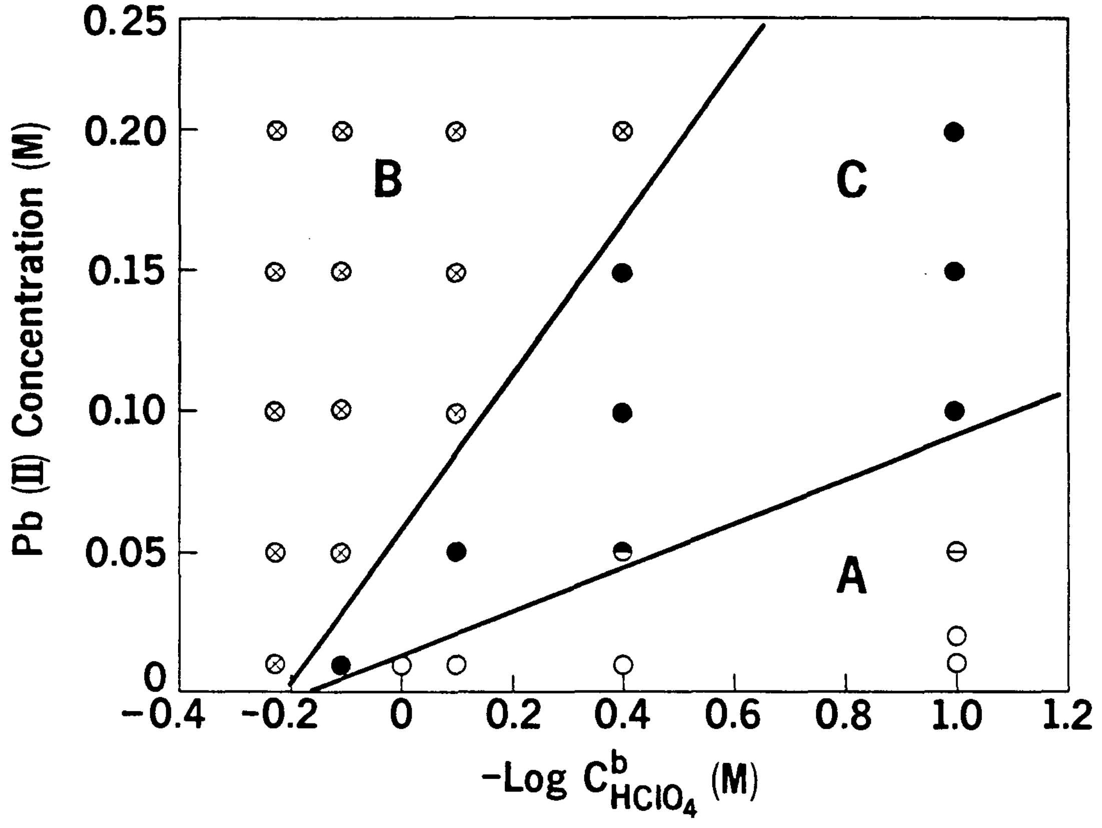

Figure 4. Dependence of the i_{ss}-$w^{1/2}$ relation on $C^b_{Pb(II)}$ and C^b_{HClO4}

If w is increased by 100%:
- (○) i_{ss} increases by 50 - 100%,
- (⊖) i_{ss} increases less than 10%,
- (◓) i_{ss} increases at low w but decreases at high w,
- (●) i_{ss} decreases,
- (⊗) i_{ss} increases by 10 - 50%

Regions:
(A) mass transport control,
(B) kinetic control,
(C) mixed kinetic-transport control

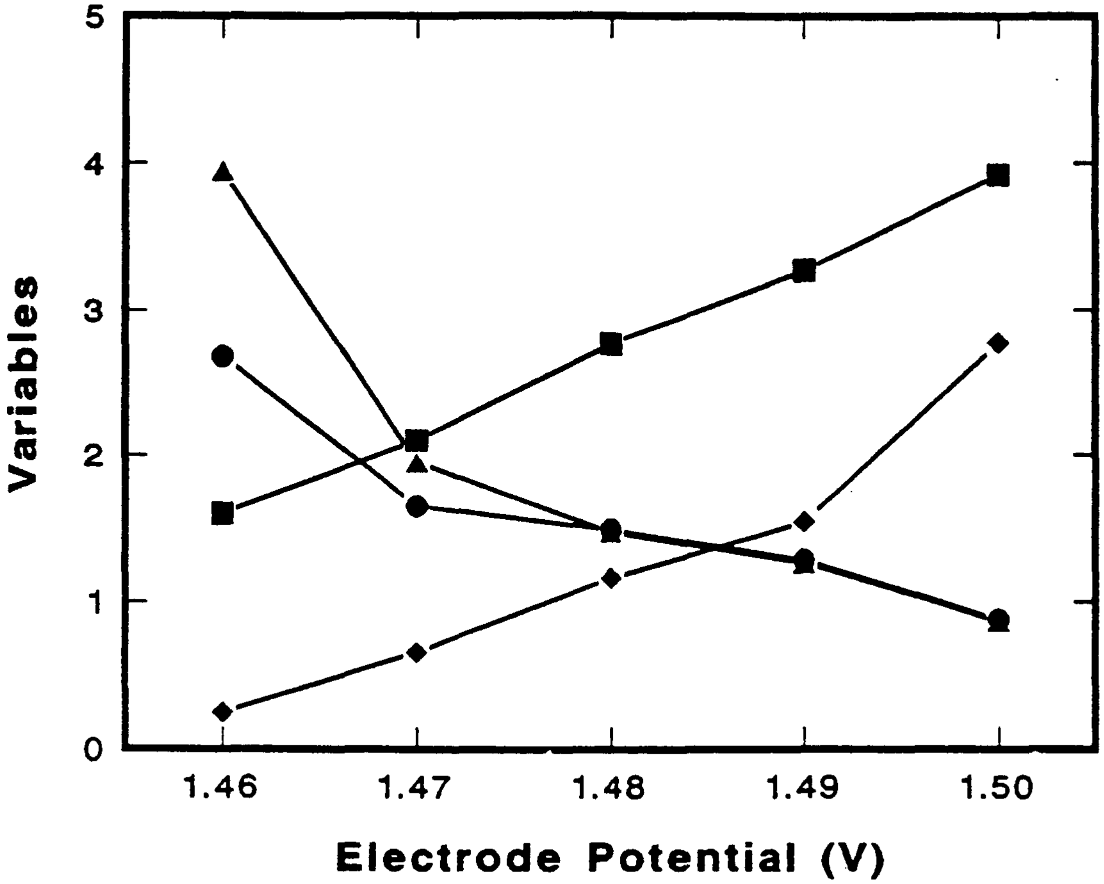

Figure 5. Plots of t_o, t_1, S and i_{ss} vs. E_{dep}

Conditions: 0.20 M Pb(II), 1.30 M $HClO_4$, 0.40 M $NaClO_4$, and 0 rev min^{-1}

Variables:
(●) t_o/2 min,
(▲) t_1/2 min,
(◆) S/0.4 mA min^{-1},
(■) i_{ss}/0.5 mA

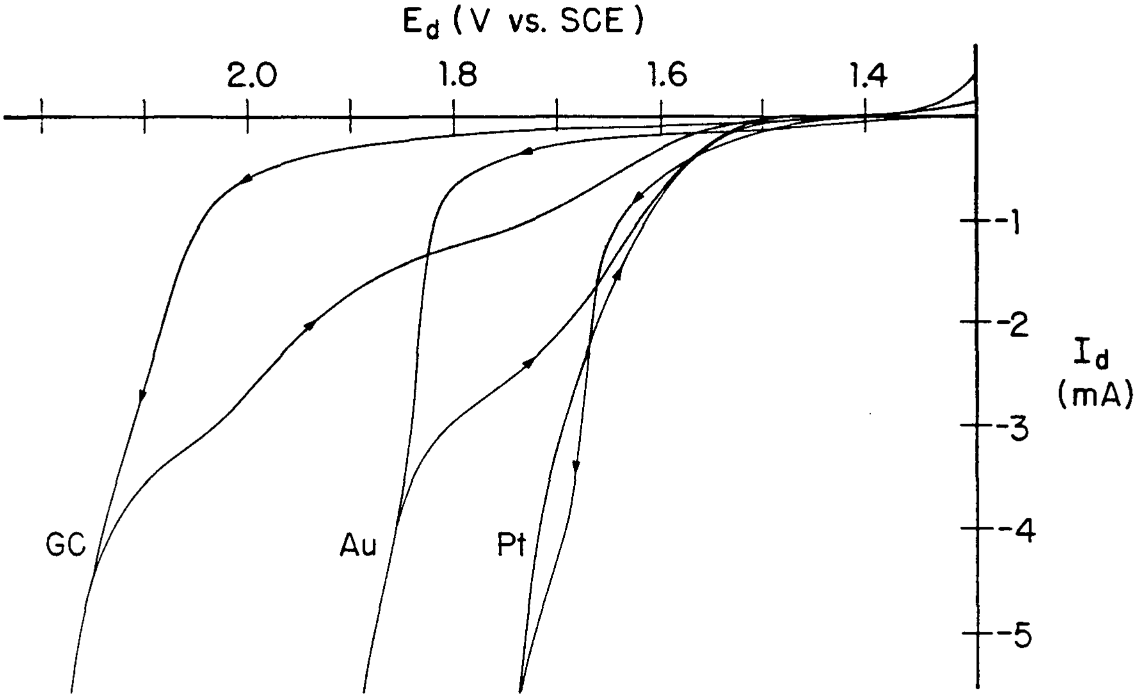

Figure 6. Cyclic voltammograms (i-E) at rotated Au, Pt and GC disc electrodes

Conditions: 10 mM Pb(II), 1.0 M $HClO_4$, 400 rev min^{-1};
scan initiated from E << 1.3 V;
scan direction indicated by arrows;
only first cyclic scan is shown

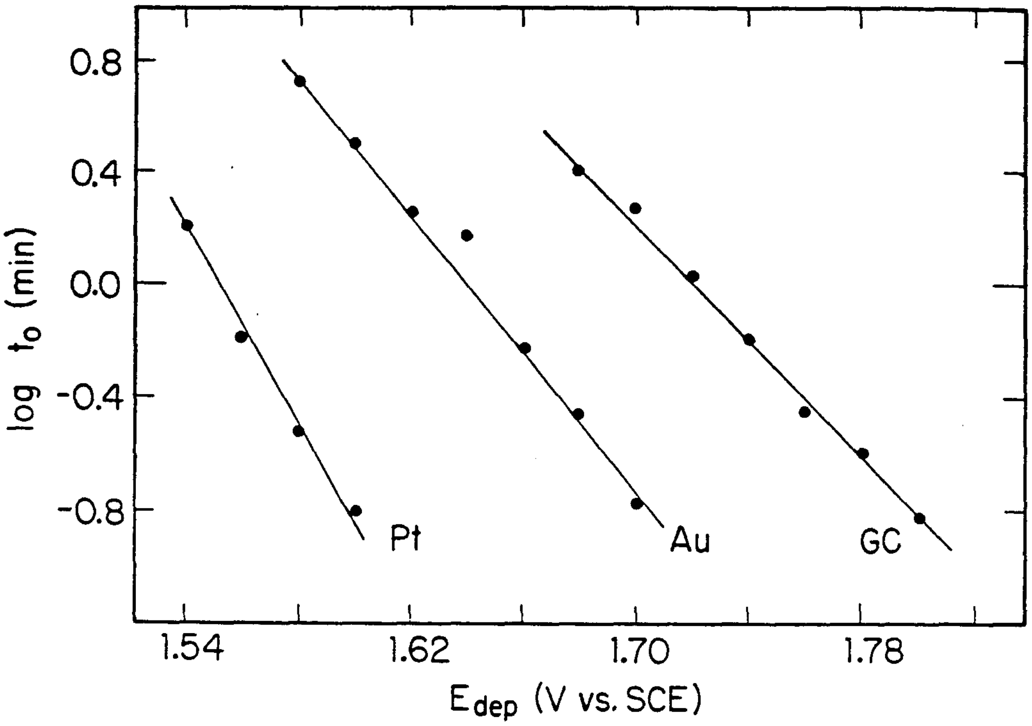

Figure 7. Plot of log t_o vs. E_{dep} for the induction period at rotated Pt, Au and GC disc electrodes

Conditions: 10 mM Pb(II), 1.0 M $HClO_4$, 400 rev min^{-1}; electrodes freshly polished prior to experiment

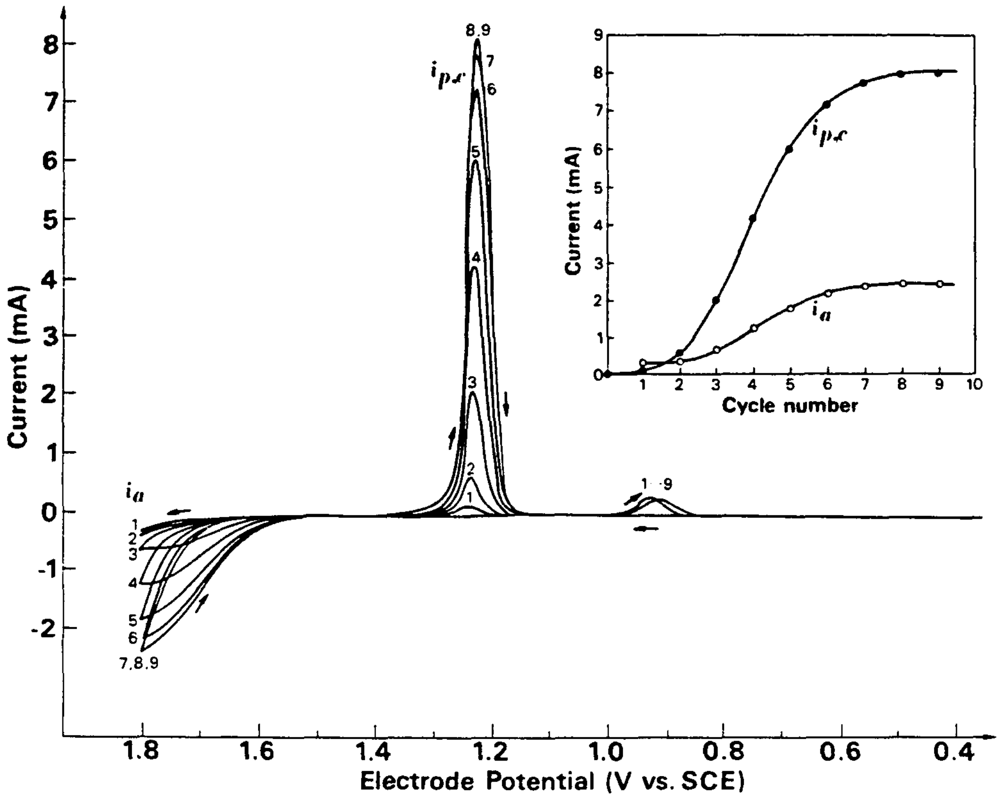

Figure 8. Cyclic voltammograms (i-E) at a rotated Au disc electrode

Conditions: 0.010 M Pb(II), 1.70 M $HClO_4$, 40 mV s^{-1}, and 1000 rev min^{-1}

Curves: cycle number as marked

Inset: i_a and $i_{p,c}$ vs. cycle number

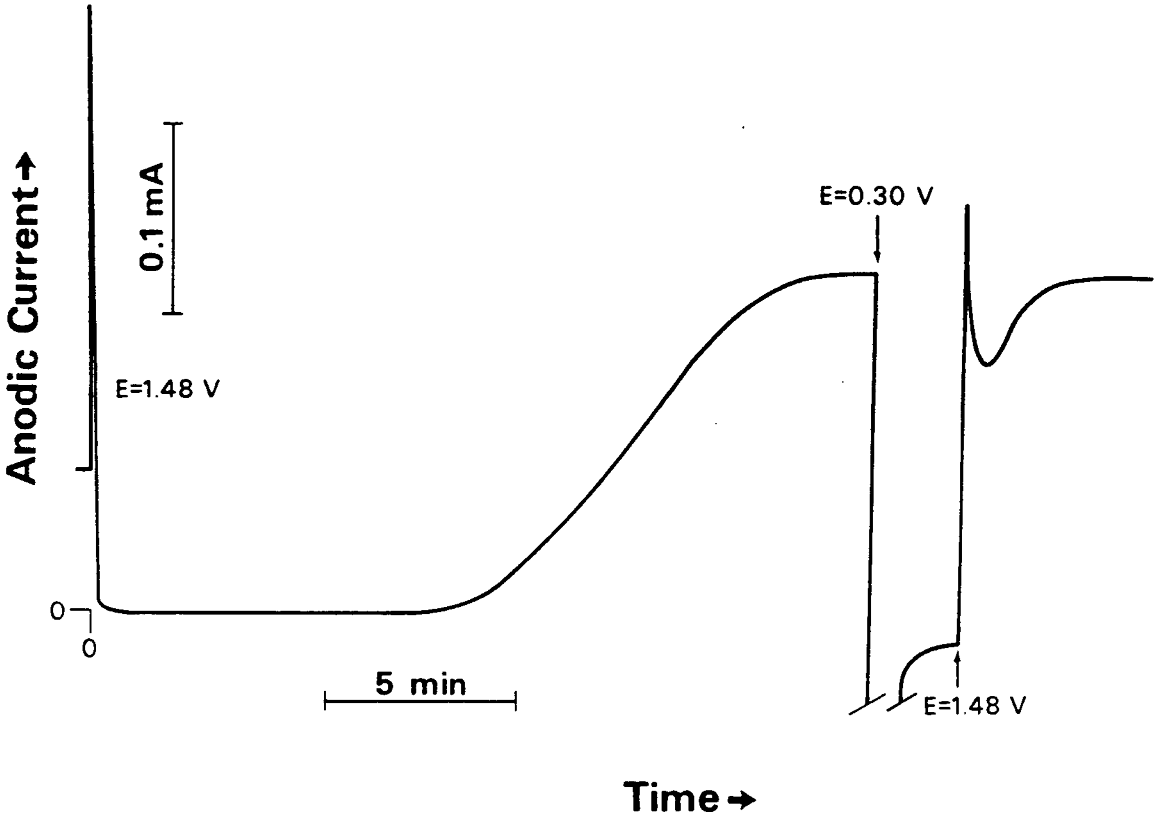

Figure 9. Chronoamperometric transients for PbO_2 deposition, stripping and redeposition

Conditions: $C^b_{Pb(II)}$ = 0.10 M, C^b_{HClO4} = 0.80 M, and 400 rev min^{-1}. E as marked

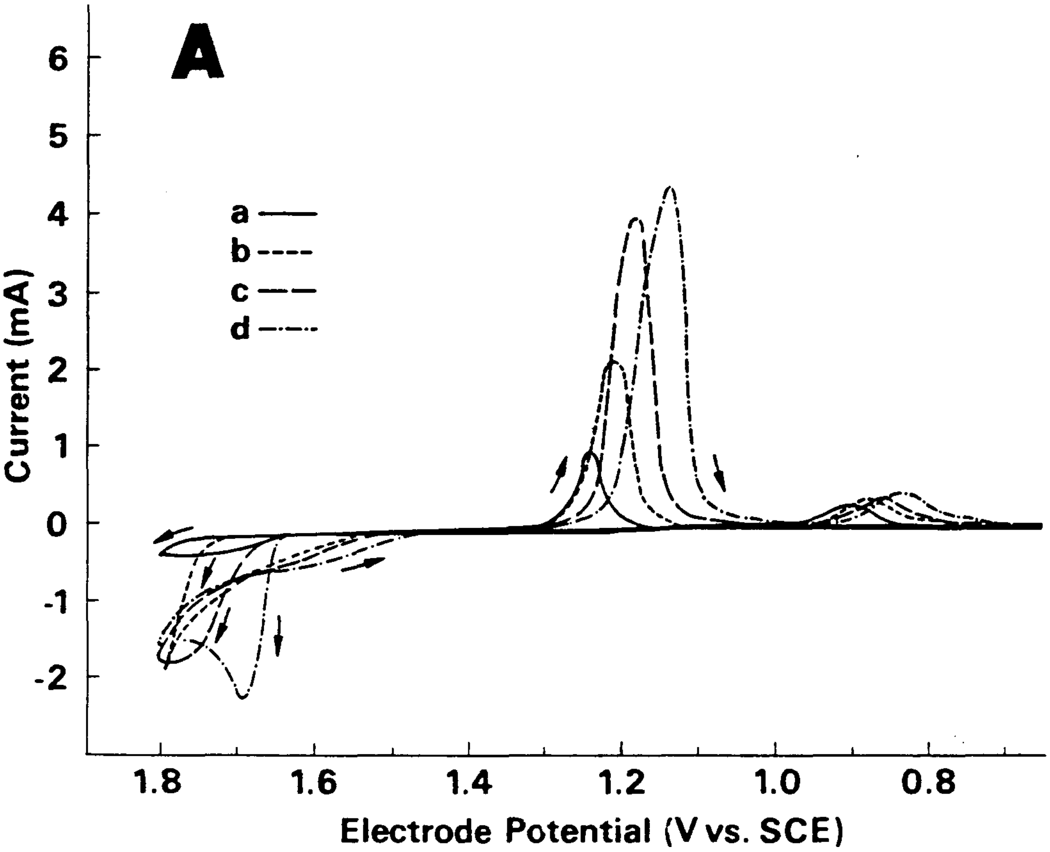

Figure 10A. Effect of pH on cyclic voltammograms: response for first cycle

Conditions: 0.010 M Pb(II), 40 mV s^{-1}, and 0 rev min^{-1}

C^{b}_{HClO4} (M): (a) 1.70, (b) 1.40, (c) 0.80, and (d) 0.40

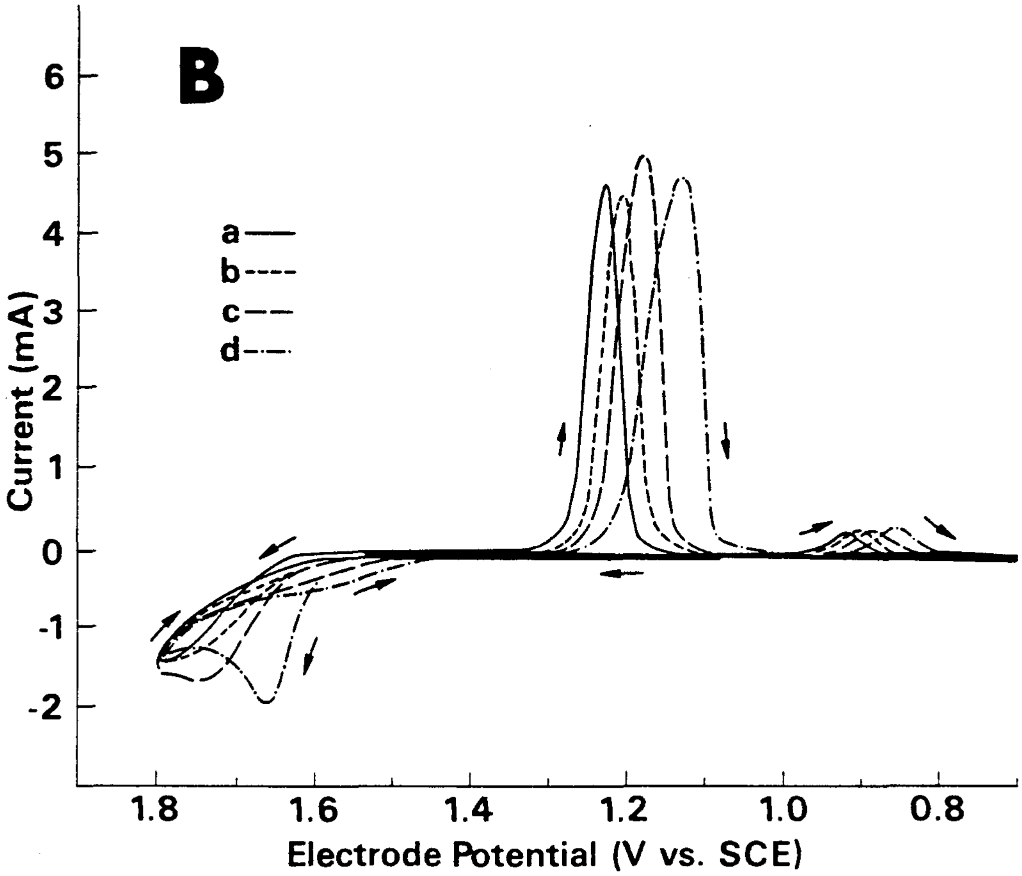

Figure 10B. Effect of pH on cyclic voltammograms: reproducible response after many cycles

Conditions: as given in Figure 10A

pp 45 - 280 removed and cycled separately -

VII. GENERAL SUMMARY

The major discoveries described in this dissertation are summarized below in correlation with the considerations in Chapter I-A.

Intermediate product for deposition and electrocatalysis at in-situ deposited PbO_2

Soluble Pb(IV) species are concluded to be generated, along with adsorbed Pb(IV) species, as intermediate products during the electrodeposition of PbO_2 in acidic media (1,2). The unstable Pb(IV) species, possibly associated with oxygen, can be used as an oxidation catalyst for some anodic oxygen-transfer reactions at in-situ deposited PbO_2 electrodes. The use of the in-situ deposited results in longer electrode lifetime than observed for pre-deposited PbO_2 (3).

Methods for chemical modification of PbO_2 surface

Modification of PbO_2 by co-deposition   A number of inorganic anions and cations can be incorporated into the PbO_2 matrix when they are present in the Pb^{2+} plating bath (4-5). This co-deposition, or electrochemical doping process, produces mixed-oxide films that behave differently from pure PbO_2. Some catalytic activities for O-t reactions were found at PbO_2 electrodes doped with Bi^{3+}, As(III), and Cl^-.

The Bi ions exposed at the surface of the Bi-doped PbO_2 can function as catalytic sites which are evenly distributed and spatially separated, as shown by EDS elemental mapping (4). This result is consistent with the proposed mechanism as shown in Figure 2 in Chapter I-A. The Bi-doped PbO_2 has higher electrochemical stability and wider voltammetric window than the pure PbO_2, probably due to the decreased alkalinity of the mixed oxide.

Modification of PbO_2 by adsorption Several ionic species, e.g., Bi^{3+}, As(V) (or As(III)), and Cl^-, can be adsorbed into the surface of PbO_2 as catalysts (5), because of the ion exchange or complexation ability of the PbO_2 surface. The adsorption method of modification has several advantages over the co-deposition method.

First, the adsorption method is more suitable for mechanistic studies. For instance, the surface concentration of Bi^{3+} at the surface of Bi^{3+}-adsorbed PbO_2 can be controlled easily by varying the bulk concentration of Bi^{3+}. A half-wave potential for the electrocatalytic oxidation reactions can be measured accurately at the Bi-adsorbed PbO_2.

Second, the co-deposition method has separate procedures for electrode preparation and testing, so is tedious and time-consuming for catalyst screening. The matter of screening is much improved with the adsorption method for which the two procedures are combined. Hence, a large number of species can be tested in a short period of time, especially if the flow-injection technique also is used (3,5b).

Mechanism of Electrocatalysis at Chemically Modified PbO_2

The mechanism of oxygen-transfer mediation described in Chapter I-A is supported by many experimental results.

Correlation between O-transfer reaction and oxygen evolution The relationship between anodic O-transfer and oxygen evolution as illustrated by Figure 1 in Chapter I-A is supported by results of the studies of anodic deposition of PbO_2 (1) and Bi-doped PbO_2 (4), and the electrocatalytic oxidation of Mn^{2+} at in-situ deposited PbO_2 (3). The deposition of the oxides occurs only in a potential region close to oxygen evolution. It is concluded that there must be enough OH species accumulated at the electrode surface, indicated by the oxygen-evolution background, to have perceptable rate of oxide nucleation.

The slight decrease of oxygen-evolution overpotential at the Bi-PbO_2 electrodes with increase in Bi coverage, as predicted in Chapter I-A, was proved for both Bi-doped PbO_2 (4) and Bi^{3+}-adsorbed PbO_2 (5a).

Effect of catalyst coverage The catalytic current for the oxidation of DMSO at Bi^{3+}-adsorbed PbO_2 electrode increases first with $[Bi^{3+}]$ at low values (5a), which is consistent with the kinetic analysis for partially covered electrodes. The mass-transport-limited values of current can be maintained only in an optimal range of $[Bi^{3+}]$. The current decreases if the $[Bi^{3+}]$ is above the optimal range due to a high value of Bi^{3+} surface coverage. This result is as predicted in Chapter 1

The catalytic activity of As(V)-adsorbed PbO_2 electrode, however, does not decrease even if the [As(V)] or [As(III)] is very high, probably because the adsorption behavior of As(V) is different from that of Bi^{3+} (5b). It is speculated that Bi^{3+} can be adsorbed more easily on PbO_2 than As(V) because of the similarity between Bi^{3+} and Pb^{4+}, so a high coverage of Bi^{3+} at PbO_2 can be built up easily.

Variation of analytes Strong activity and high current efficiency at the modified PbO_2 electrodes were observed for many practically important electrolytic processes, besides the model reactions, e.g., oxidation of Cr(III) to chromic acid and of benzene to benzoquinone.

The same $E_{1/2}$ value was obtained at the Bi^{3+}-adsorbed PbO_2 electrode for a large variety of O-t reactions (5b), despite the large difference in their standard potentials. This result is consistent with the prediction in Chapter I-A. It is concluded that this $E_{1/2}$ value is associated with the discharge of water to generate the adsorbed OH species at the catalytic sites of the modified electrode surface.

Variation of catalysts The $E_{1/2}$ values are almost the same for Bi^{3+} and As(V) (or As(III)), while the E° values for the Bi^{3+}/Bi^{5+} and As(III)/As(V) couples are far apart, at ca. 1.8 and 0.32 V vs. SCE, respectively. Therefore, it is concluded that the electrocatalysis at the modified PbO_2 electrodes does not occur via electron-transfer mediation but via oxygen-transfer mediation, and the catalyst at the electrode surface does not have to undergo any redox process. However, the electrocatalytic activity of Cl^-- and Ag^+-modified PbO_2 electrodes are lower than that of the Bi^{3+}- and As(V)-modified PbO_2, which is concluded to be due to the difference in the affinity of the catalysts to hydroxide radicals.

Use of modified PbO_2 to modify other solid electrodes

Modified PbO_2 films can be used to modify other conventional, inert solid electrodes (6). Consecutive deposition and stripping of Bi-doped PbO_2 at Au, Pt, GC, and Ti produced ultra-thin films of the mixed oxides on the substrates (6). The ultra-thin Bi-PbO_2 film-covered electrodes have higher electrochemical stability and catalytic activity than the thicker, normal film electrodes, due to an enhanced surface concentration of Bi.

Deposition of smooth, non-porous PbO_2 film with low residual signal

In order to use the pure and modified PbO_2 film electrodes in electroanalytical devices, the residual signal at the electrode should be as small as possible. A capacity residual current was observed to be proportional to the surface roughness or porosity of the PbO_2 film (4). A smooth, reflective, and compact PbO_2 film can be deposited on Au and Pt substrates under the optimized conditions (1). Electron micrgrph showed that the surface of this PbO_2 film was smooth on a micrometer scale (6a). The residual current at this PbO_2 film was very small (4), which was also true after modification by Bi^{3+} adsorption (6a). As shown by XRD, the PbO_2 film deposited in this way has a small crystalline size (6b), due to a very fast rate of nucleation and growth.

References

1. Chang, H.; Johnson, D. C. J. Electrochem. Soc. 1989, 136, 17; Chapter II-A, this Dissertation.

2. Chang, H.; Johnson, D. C. J. Electrochem. Soc. 1989, 136, 23; Chapter II-B, this Dissertation.

3. Chang, H.; Johnson, D. C., in preparation; Chapter III-A, this Dissertation.

4. Chang, H.; Johnson, D. C. In preparation; Chapter III-B, this Dissertation.

5. (a) Chang, H.; Johnson, D. C., in preparation; Chapter IV-A, this Dissertation. (b) Chang, H.; Johnson, D. C., in preparation; Chapter IV-B, this Dissertation.

6. (a) Chang, H.; Johnson, D. C., in preparation; Chapter V-A, this Dissertation. (b) Chang, H.; Johnson, D. C., in preparation; Chapter V-B, this Dissertation.

VIII. SUGGESTIONS FOR FURTHER STUDIES

Answers to the questions in the present research always lead to many new questions for studies in the future.

Applications of chemically modified PbO_2 electrodes

The most important application of the modified PbO_2 electrodes is predicted to be in the area of large-scale electrolysis, e.g., electrosynthesis. Further studies are needed for up-scaling of the electrolytic processes already tested. Many more O-t reactions also can be studied.

Another application will be in the area of electrochemical transducers. Substances whose oxidation reactions are too slow at conventional electrodes can be detected at these new catalytic electrodes.

Mechanism of oxygen-transfer mediation

The mechanism of electrocatalysis at the modified PbO_2 electrodes is of fundamental importance. To further prove the mechanism of O-t mediation, some in-situ analytical methods, e.g., electron-spin resonance (ESR), infrared spectroscopy, scanning tunneling microscopy (STM), and Raman spectroscopy, can be used to monitor the changes of the electrode surface during the electrolysis. Kinetic analysis with digital simulation can be used to verify the mechanism with kinetic data.

Much information concerning the mechanism can also be obtained by a better understanding of the causes for the differences in catalytic activity among the Bi-doped, Bi-adsorbed, and Bi-doped ultra-thin-film

PbO_2 electrodes. It remains as a question whether the surface lead and oxygen species participate in the electrocatalysis.

Studies also can be conducted to understand more about the kinetics and mechanism of the adsorption of ionic species at the PbO_2 electrode, including a direct measurement of the surface concentration of the catalyst with surface analytical techniques.

Photocatalysis

The photocatalytic phenomenon at the supported PbO_2 can be the subject of future study, including a quantitative measurement of the rate of the photocatalytic reaction and the conductivity of the PbO_2 film as a function of preparation conditions. More reactions can be studied beside the oxidation of Mn^{2+} to MnO_2. It is expected that the conductivity of the PbO_2 will be changed by doping with bismuth, so will the photocatalytic activity. Attention also can be paid to the photoelectrochemical reactions at the pure and modified PbO_2 electrodes. These results will yield information for comparison of electrochemical and photocatalytic O-t reactions.

IX. ACKNOWLEDGMENT

It was accidental that I chose Iowa State for my Ph.D. study and Prof. Dennis C. Johnson as my major advisor. However, now had I been given ten more chances to choose, I would still have made the same choices. I am in debt to Prof. Johnson especially for his genuine guidance, extreme patience, and endless courage throughout the four years and much more to come. He has become a life-time role-model for me, both as a scientist and as an individual.

Special thanks are due to James Anderegg for assistance to obtain XPS results, Glen Oren and Jerry Amenson for SEM and EDS, Scott Schlorholtz for XRD, Stephen Veysey and Jan Beame for GC/MS, and Roger Jones and John McClelland for FTIR.

I would like to thank other members of the group with whom I have worked, especially, Brian Wels-"Mr. Deionized Water," Andy Tang-"Mr. Answer," Bill LaCourse, In-Hyong Yeo, Larry Larew, Jianren Feng, Yun-Lin Hsiao, and Brian Issac. I'll miss you.

Assistance and good jobs are greatly appreciated from the people in the Machine Shop, Glass Shop, and Storeroom of the chemistry department.

This research was supported by Ames Laboratory of the U. S. Department of Energy. It also was made possible partially by the teaching assistantship provided to me by the chemistry department.

I want to thank my family for their constant support to my "long-term" education. Finally, my life in Ames would have been impossible without my wife and companion, Suichu. By her love and understanding, she made it all possible with some sacrifices on herself.